International Atomic Energy Agency

INDC(ROM)-020/LJ

INDC INTERNATIONAL NUCLEAR DATA COMMITTEE

PRE-EQUILIBRIUM EMISSION AND NUCLEAR LEVEL DENSITIES IN NEUTRON INDUCED REACTIONS ON Fe, Cr AND Ni ISOTOPES

M. Ivascu, M. Avrigeanu, I. Ivascu and V. Avrigeanu
Institute of Physics and Nuclear Engineering
Bucharest, Romania

This work was performed under IAEA Research Contract 3802

January 1989

IAEA NUCLEAR DATA SECTION, WAGRAMERSTRASSE 5, A-1400 VIENNA

INDC(ROM)-020/LJ

PRE-EQUILIBRIUM EMISSION AND NUCLEAR LEVEL DENSITIES IN NEUTRON INDUCED REACTIONS ON Fe, Cr AND Ni ISOTOPES

M. Ivascu, M. Avrigeanu, I. Ivascu and V. Avrigeanu
Institute of Physics and Nuclear Engineering
Bucharest, Romania

This work was performed under IAEA Research Contract 3802

January 1989

Reproduced by the IAEA in Austria
January 1989

89-00221

PRE-EQUILIBRIUM EMISSION AND NUCLEAR LEVEL DENSITIES IN NEUTRON INDUCED REACTIONS ON Fe, Cr and Ni ISOTOPES *)

M.Ivaşcu, M.Avrigeanu, I.Ivaşcu and V.Avrigeanu
Institute for Physics and Nuclear Engineering, Bucharest, Romania

A b s t r a c t

The experimentally well known (n,p), (n,α) and (n,2n) reaction excitation functions, from threshold to 20 MeV incident energy, and neutron, proton and alpha-particle emission spectra at 14.8 MeV from Fe, Cr and Ni isotopes are calculated in the frame of a generalized Geometry-Dependent-Hybrid pre-equilibrium emission model, including angular momentum and parity conservation and alpha-particle emission, and the Hauser-Feshbach statistical model. Use of a consistent statistical model parameter set enables the validation of the pre-equilibrium emission model. Moreover, an enhanced pre-equilibrium emission from higher spin composite system states, associated with higher incident orbital momenta, has been evidenced. Higher orbital momenta involved also in the emergent channels of this process are suggested by calculations of the residual nuclei level populations. Finally, the unitary account of the (n, p) and (n, 2n) reaction excitation functions for Fe, Cr and Ni isotopes has allowed the proper establishment of the limits of the transition excitation range between the two different nuclear level density models used at medium and higher excitation energies, respectively.

1. I N T R O D U C T I O N

In the frame of the IAEA Coordinated Research Programme on "Methods for the Calculation of Fast Neutron Nuclear Data for Structural Materials" (1986-1988) the IPNE group have planned the completion of the (n, p), (n, n'p), (n, α), (n, n'α), (n, 2n) and (n,3n) reaction cross section calculations for all stable isotopes of Fe, Cr and Ni elements, in the energy range from threshold to 20 MeV, in the frame of the pre-equilibrium emission Geometry-Dependent Hybrid (GDH) model [1] and the Hauser-Feshbach-Moldeauer statistical model [2,3]. The unitary account of a so abundant experi-

---

*) Work presented at the 2nd Meeting of the IAEA Coordinated Research Programme on "Methods for the Calculation of Fast Neutron Nuclear Data for Structural Materials", IAEA Vienna, February 15-17, 1988.

mental data base has been thought as a proper validation of the nuclear models employed.

In the first year (1986) the accomplished objectives were: (a) the development of the GDH model through the inclusion of the angular momentum and parity [4], (b) the establishment of nuclear level density models and parameters as more accurate and realistic as possible [5], and (c) the analysis of the gamma-ray strength functions used for the gamma-ray transmission coefficient calculations [6]. The second year (1987) of the project has been devoted to the appropriate validation of the improved pre-equilibrium emission model and the previously analysed statistical model parameters through the calculation and comparison with the experimental data of some well experimentally known particle emission spectra and reaction excitation functions of interest.

The unified description of the pre-equilibrium and equilibrium processes is being fully achieved by the more rigorous quantum-approaches of the pre-equilibrium emission. However, the numerous approximations yet under investigation make these theories less suitable for applied purposes. On the other hand, to consistently involve a semi-classical pre-equilibrium model into a Hauser-Feshbach model calculation, the angular momentum and parity conservation has to be considered also in the first stage of the reaction. This aspect has been taken into account within the GDH model [4], in the frame of the computer code STAPRE-H [7]. To validate the proposed approach, the experimentally well known neutron, proton and alpha particle emission spectra from $^{54,56}Fe$ targets are calculated and discussed in the present work. The statistical model parameters have been mainly determined or validated by means of various independent types of experimental data.

In the first instance the alpha-particle emission has been analysed, although not described by the GDH model, to assure the accounting of the all available experimental data. To this extent the alpha-particle pre-equilibrium emission has been calculated in the frame of the exciton model, whose free parameter has been derived fitting the particle emission data. However, the resulted importance of the pre-equilibrium alpha-particle emission for an accurate cross section calculation determined the accounting of also this process in the frame of a generalized GDH model. The hypothesis of the Milano group [8-10] on the preformed alpha-particle existence in the nucleus has been followed in this respect.

The last main goal of this work consists in the establishment of the limits of the transition excitation range between the two different nuclear level density models used at medium and higher excitation energies, respectively. These limits are the only free statistical model parameters which are obtained from the analysis of the experimental cross section data. While the agreement of the calculated and experimental data in the low energy part of the (n,p) and (n,α) excitation functions is validating the other statistical model parameters, the same agreement at incident energies above 10 MeV have been obtained by the appropriate choice of the transition excitation range limits for the nuclear level density models. This goal has been properly attained through an unitary account of a whole body of related data, respectively the experimentally well known (n,p) and (n,2n) reaction excitation functions for Fe, Cr and Ni isotopes.

Finally, the accomplishment of these objectives is validating both the pre-equilibrium emission model employed and the calculation methods to be used in extensive calculations of structural material fast neutron data.

2. THE GENERALIZED GDH MODEL INCLUDING ANGULAR MOMENTUM AND PARITY CONSERVATION AND α-PARTICLE EMISSION

Following both the inclusion of the J^{π} - conservation and the energy dependent single-particle level density accounting [4], the differential emission spectrum of a particle x within the channel energy ε to ε + dε looks like:

$$\frac{d\sigma_x(\varepsilon)}{d\varepsilon} = \pi\lambda\!\!\!^{-2} \sum_{J,\pi} g_J \sum_{\ell} T^J_{\ell} \sum_{n} \sum_{\ell'} \sum_{I',\pi'} \left[{}_n p_x \cdot \frac{\rho_n(p,h,U,\varepsilon,I')}{\rho_n(p,h,E,J)} \right] \cdot$$

$$\cdot \frac{\frac{1}{2\pi\hbar} \cdot \frac{1}{g(\varepsilon+B_x)} \cdot (2i'_x+1).(2\ell'+1).T^J_{\ell'}(\varepsilon)}{\sum_{\ell'} \sum_{J',\pi'} \frac{1}{2\pi\hbar} \cdot \frac{1}{g(\varepsilon+B_x)} \cdot (2i'_x+1)(2\ell'+1).T^J_{\ell'}(\varepsilon)+(2J+1)\lambda_{n+2,x}(\varepsilon)} \cdot D_n^{J^{\pi}} \qquad (1),$$

where E and U are the excitation energies of the n-excitons composite system and residual nuclei, respectively, and T^J and $T^J_{\ell'}$ are the transmission coefficients for the incident and emergent channels characterized by the coupling scheme:

$$\vec{J} = (\vec{I} + \vec{i}) + \vec{\ell} = (\vec{I}' + \vec{i}'_x) + \vec{\ell}' \qquad (2)$$

The spin dependence of the particle-hole level density $\rho_n(p,h,E,J)$ has been described by means of the simplified representation of Fu [11]. Moreover, the one-fermion type exciton-state densities previously employed [4] have been transformed into two-fermion-like densities using the renormalization procedure of Akkermans and Gruppelaar [12]. The energy dependence of the single-particle level density g has been given by the energy dependent nuclear level density parameter $\underline{a}$ (E) used in the Hauser-Feshbach model calculations at higher excitation energies [4] through the usual relation

$$g = \frac{6}{\pi^2} \underline{a} .$$

The intra-nuclear transition rates $\lambda_{n+2,x}(\varepsilon)$ have been calculated employing the same imaginary optical model potentials as in the statistical model calculations. The last factor of (1), $D_n^{J^\pi}$, is the depletion factor that reduces the population of each exciton state according to the amount of particle emission from simpler exciton states.

The specific problems connected with the accounting of the pre-equilibrium emission of alpha-particles in the frame of the hybrid model were pointed out by Chevarier et al. [13] when simultaneously analysed the neutron, proton and alpha-particle spectra induced by 25.6 MeV ^{3}He incident on A ≈ 60 mass target nuclei. As well as the Milano group assumed in the frame of the exciton model analyses of nucleon induced reactions [8-10], the emission of alpha-particles has been considered a pre-equilibrium process of an alpha-particle existing preformed in the nucleus. Actually, one has to take into account a probability that four correlated nucleons exist in a alpha-particle-like configuration which is excited during the nuclear process. Therefore it is assumed that this preformed alpha-particle can be treated as an exciton having the single-particle state density g/4 and being emitted from n-exciton states, starting with n = 3. Following the same hypotheses, the following expression has been derived from (1) for the alpha-particle emission in a generalized GDH model:

$$\frac{d\sigma_\alpha(\varepsilon)}{d\varepsilon} = \pi\lambda\!\!\!^{-2} \sum_{J,\pi} g_J \sum_{\ell} T_\ell^J \sum_n \sum_{\ell'} \sum_{I',\pi'} \cdot \left[\frac{\varphi K^\alpha_{p-1,h}}{\varphi K^\alpha_{p,h} + (1-\varphi) K^\nu_{p,h}} \cdot \frac{\rho_n(p,h,U,\varepsilon,I')}{\rho_n(p,h,E,J)} \right] \cdot$$

$$\cdot \frac{\frac{2\ell'+1}{2\pi\hbar} \cdot \frac{1}{g(\varepsilon+B_\alpha)} \cdot T^J_{\ell',\alpha}(\varepsilon)}{\sum_{\ell'} \sum_{I',\pi'} \frac{2\ell'+1}{2\pi\hbar} \cdot \frac{1}{g(\varepsilon+B_\alpha)} \cdot T^J_{\ell',\alpha}(\varepsilon) + (2J+1)\lambda_{n+2,\alpha}(\varepsilon)} \cdot D_n^{J^\pi} \qquad (3)$$

The coefficients $K^{\alpha}_{p,h}$ and $K^{\nu}_{p,h}$ defining the n-exciton state densities in the case of the excitation of an alpha-particle with the probability φ and otherwise of a nucleon ν [8] have been taken as given by Gadioli et al. [9]. The probability φ has been established by means of the comparison of the experimental and calculated alpha-particle spectra. Similarly to the nucleon emission treatment, the intra-nuclear transition rates $\lambda_{n+2,\alpha}(\varepsilon)$ have been evaluated starting from the mean free path of alpha-particles in nuclear matter and using the optical model potential parameters involved in the calculation of the transmission coefficients $T^{J}_{\ell',\alpha}(\varepsilon)$.

3. Fe ISOTOPES

3.1. *NUCLEAR MODEL PARAMETERS*

The prediction capability of the fast neutron cross section calculations is closely related to the use of as few as possible free parameters. The GDH model has no its own such parameter. However, some of its characteristic elements are connected with the statistical model parameters. A consistent set of input parameters had to be determined or validated using in the lowest degree the analysed reaction cross section data.

The nuclear level densities have been described by means of the empirical back-shifted Fermi gas (BSFG) model [14], at medium excitation energies, and of the realistic analytical formula of Schmidt et al. [15] at the higher excitation energies. The BSFG parameters redeterminated [5] by a least-squares fit of recent experimental total numbers of the low-energy discrete levels and s-wave neutron resonance spacings have been used. In [5] giving also the discrete level numbers and the corresponding upper excitation energies considered in the Hauser-Feshbach calculations, are discussed more widely both the need to choose a more realistic level density representation at higher excitations and the Schmidt et al. [15] formula. This one, employing microscopic suggested parameters, although does not take into account the collective effects in the nuclear level density is in a rather good agreement with the phenomenological formula of Ignatyuk et al. [16]. While the use of any of these formulas, characterized by an energy dependent level density parameter $\underline{a}(E)$, is able to solve the noticed ambiguities in the application of the statistical model at quite higher excitations as involved in heavy ion induced reactions [17], in the calculations specifically to fast neutron

induced reactions is also important the transition range between the BSFG model and the higher energy realistic formula. The previous analysis [5] has suggested the excitation energy range from neutron binding energy to about 25 MeV, where a linear interpolation between the spin dependent level densities as well as between the a values given by the two different models at the transition range limits has given the related quantities. Furthermore, these limits have been checked in the frame of the present (n,p) and (n,2n) reaction excitation function calculations.

Neutron transmission coefficients were derived from the spherical optical model potential (OMP) parameters of Arthur and Young [18], obtained by means of a simultaneous fit of the (a) S_0 and S_1 strength functions and potential scattering radii, (b) total neutron cross sections from 20 to 40 MeV and (c) elastic scattering angular distributions from 6.0 to 14 MeV, and confirmed [19] through the analysis of the elastic and inelastic scattering angular distributions from 6.0 to 14 MeV, for ^{54,56}Fe target nuclei.

Proton transmission coefficients given by the OMPs of Arthur and Young [18] and Kailas et al. [20] (global set) have been used for ^{56}Mn and ^{54}Mn nuclei, respectively. The first set was derived from the global OMP parameter set of Perey [21] to better fit low energy data as well as (p, n) and (p, 2n) reactions on ^{56}Fe for incident energies from 10 to 40 MeV. Kailas et al., looking for the consistency of the low and high energies optical model predictions, analyzed (p, n) reaction excitation functions of nuclei from ^{45}Sc to ^{80}Se at incident energies below ≃ 5 MeV and finally derived a global set of OMP parameters in the proton energy range between 4 and 180 MeV, for medium weight nuclei.

Alpha-particle transmission coefficients have been calculated using the OMPs derived by Arthur and Young [18], adjusted to better fit the low energy (α, n) data, and McFadden and Satchler [22], for ^{53}Cr and ^{51}Cr nuclei, respectively. Both are giving related reaction cross sections, the latter one being conclusively proved [23] as preferably against the OMP of Huizenga and Igo [24].

Gamma-ray transmission coefficients have been derived from the gamma-ray strength functions in the usual way. For the

electric dipole radiation dominant transition the giant dipole resonance model with modified [25] energy-dependent Breit-Wigner line shapes [26] has been used.

A *fraction* $f^{\alpha}_{PE} = \sigma^{\alpha}_{PE}/\sigma_R$ for the pre-equilibrium emission of the alpha-particles has been used to reduce more the compound nucleus formation cross section when the accounting of this process has been performed in the frame of the exciton model. Its consideration compensates the shortcoming of the GDH model concerning the alpha-particle emission. For the evaluation of this fraction the exciton model, initially included in the code STAPRE, has been employed. The options $g \simeq A/13$ and pairing accounting for particle-hole state densities, and the $\varphi = 0.2$ value for the α - cluster preformation factor were used. The free parameter K of the internal transition matrix element has been derived analyzing the proton emission spectra at $E_n \simeq 14.8$ MeV and the (n,p) reaction excitation functions. A value of 180 MeV^3 has given a better agreement between the calculated and experimental data, in rather good agreement with 160 MeV^3 [18].

The atomic masses and Q-values were taken from [27] and energy bin-sizes of 0.3 and 0.4 MeV were used for lower and higher incident energies than $E_n \gtrsim 15$ MeV, respectively.

3.2. RESULTS OF CALCULATIONS

The goals of this part of work have been (a) the feasibility test of the modified GDH model based calculations to reproduce a large body of correlated data and (b) the analysis of the physics revealed by the angular momentum inclusion in the pre-equilibrium emission account. Therefore, the numerous types of data existing for the fast neutron induced reactions on ^{54}Fe (Figs. 1-4) and ^{56}Fe (Figs. 5-7) isotopes have been chosen for the validation of both the statistical model parameters employed and the GDH model predictions.

The (n,p) reaction excitation functions (Figs. 1-5) have proved the adequacy of the low-energy proton transmission coefficients by means of the agreement between the experimental and calculated data on their first few MeV-s. When necessary the width fluctuation correction [3] was used, with the fluctuation parameter $\nu = 2$. At this point the $^{54}Fe(n,p)^{54}Mn$ data determined the accounting of the proton OMP of Kailas et al. [20], the parameter set of Arthur and Young [18] leading to calculated cross sections within ≈25% higher than the experimental ones. Above

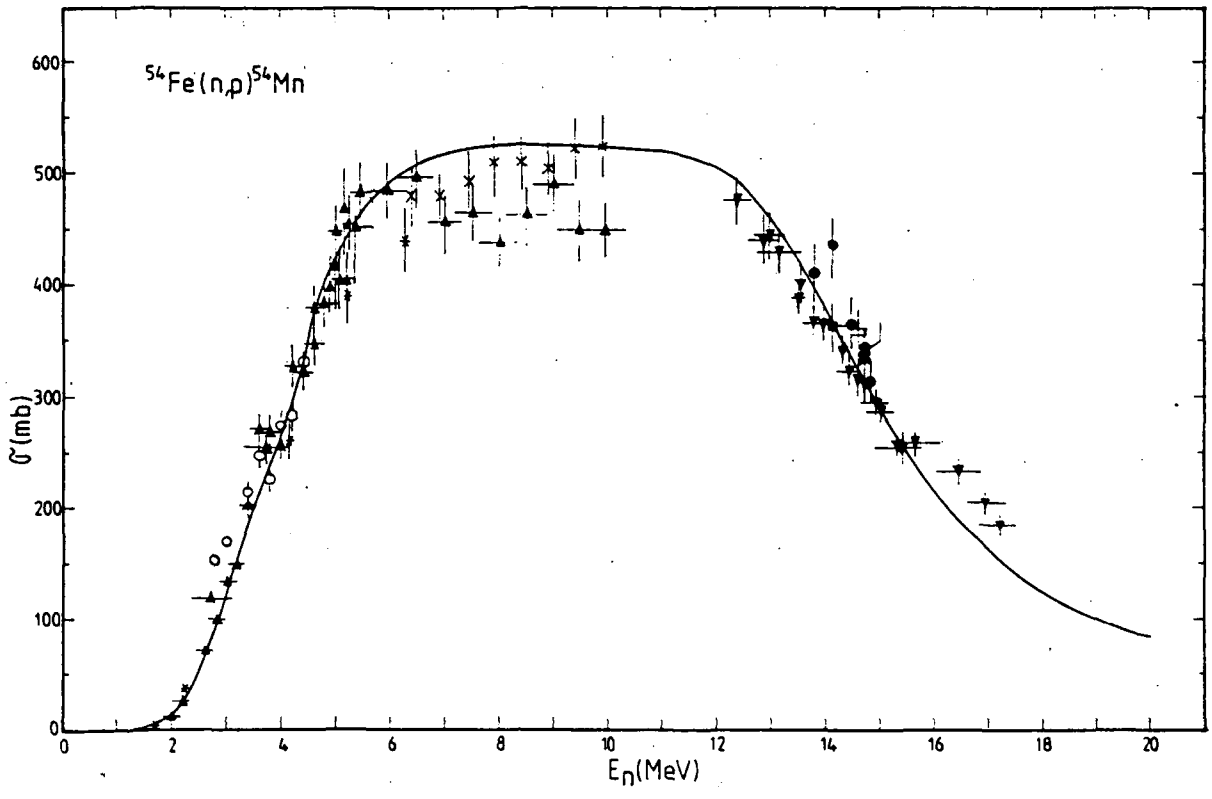

Fig. 1. Comparison of experimental cross sections of the reaction $^{54}Fe(n,p)^{54}Mn$ and calculated values within the pre-equilibrium emission model GDH, including angular momentum and parity conservation, and Hauser-Feshbach statistical model (——). Experimental data: ✱ [33], ✱ [34], ▲ [35], o [36], ■ [37], × [38], ■ [39], ▼ [40], • [41] (numerical data are from the computerized exchange format EXFOR [42] files).

Fig. 2. The same as Fig. 1, for the reaction $^{54}Fe(n,\alpha)^{51}Cr$, with supplemental curve (-·-·-) obtained through the addition of the pre-equilibrium emitted alpha particle cross section σ^{α}_{PE}, calculated within the exciton model, to the statistical cross section $\sigma_{HF,(n,\alpha)}$ (Fig.2a). The statistical and generalized GDH model predictions for probability φ values 0.2 (full curve) and 0.3 (dashed curve) are compared with exciton model with φ = 0.2 (dotted curve). (Fig.2b). Experimental data: o [43], ■ [37], ▼[40], ■ [44].

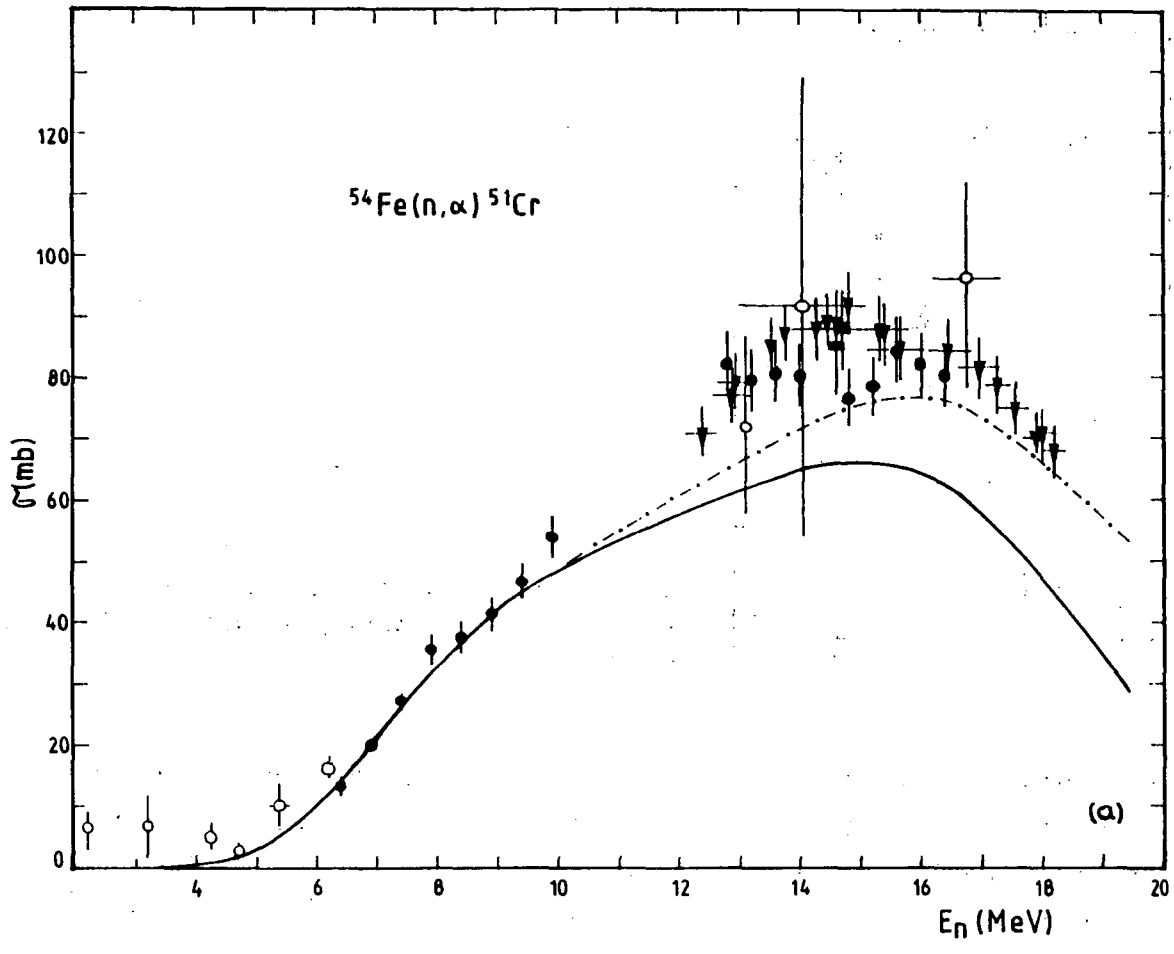
$^{54}Fe(n,\alpha)^{51}Cr$
σ(mb)
E_n (MeV)
(a)

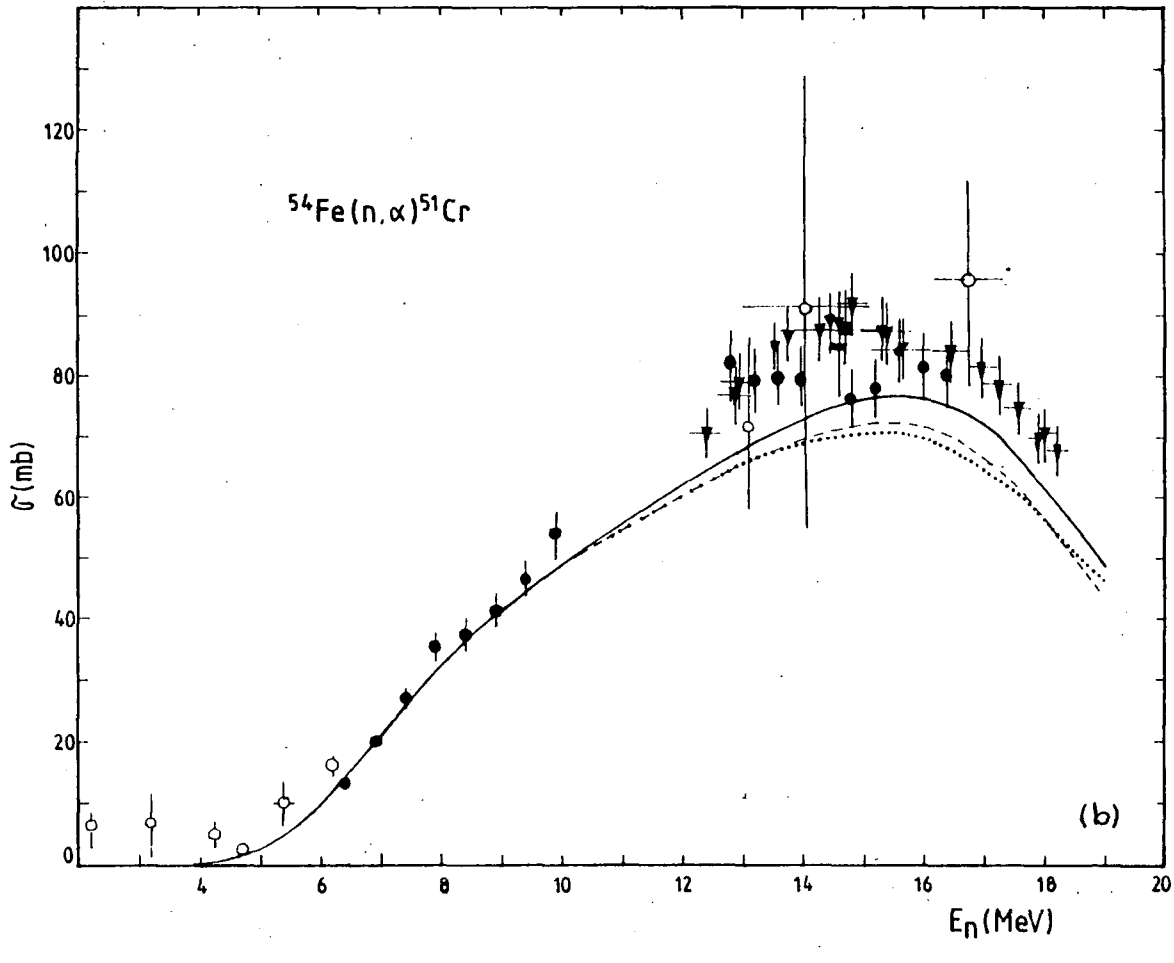
$^{54}Fe(n,\alpha)^{51}Cr$
σ(mb)
E_n (MeV)
(b)

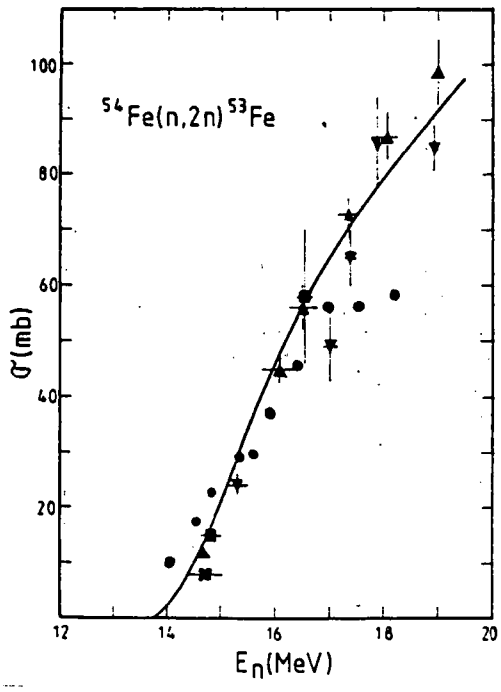

Fig. 3
Same as Fig. 1, for the reaction $^{54}Fe(n,2n)^{53}Fe$. Experimental data: ✱ [45], ■ [46], • [47], ▲ [48], ▼ [49].

this energy range the nuclear level densities of the dominant neutron and proton channels start to play their important role. Moreover, the higher energy parts ($E_n \gtrsim 12$ MeV) are enlightening the correctness of the transition excitation range limits between the models involved in the level density description.

The last aspect is also common to the *(n, 2n) reaction excitation functions* (Figs. 3-6). Their yet increasing trend at $E_n = 20$ MeV is particularly sensitive to the variation of the transition higher limit [9]. Based on the analysis of these four excitation functions as well as other similar data for Cr, Ni and Ti isotopes [28], the excitation transition range ≈8 - ≈30 MeV has been established. On the other hand, the agreement of the calculated (n, 2n) reaction cross sections with the experimental ones nearly the reaction threshold substantiated both the low-energy neutron transmission coefficients and the γ - ray competition accounting.

The $^{54}Fe(n,\alpha)^{51}Cr$ reaction excitation function has been calculated (Fig. 2) in order to confirm the statistical model parameters for all channels. Because of the pre-equilibrium emission character of the most energetic alpha particles, proved by the angular distribution study [29], the alpha particle pre-equilibrium emission has been analysed within both the exciton model (cfm. Sect. 2) and the generalized GDH model. In the first case the corresponding cross section σ^{α}_{PE} has given the fraction f^{α}_{PE} of the absorption cross section, further used in the establishing of

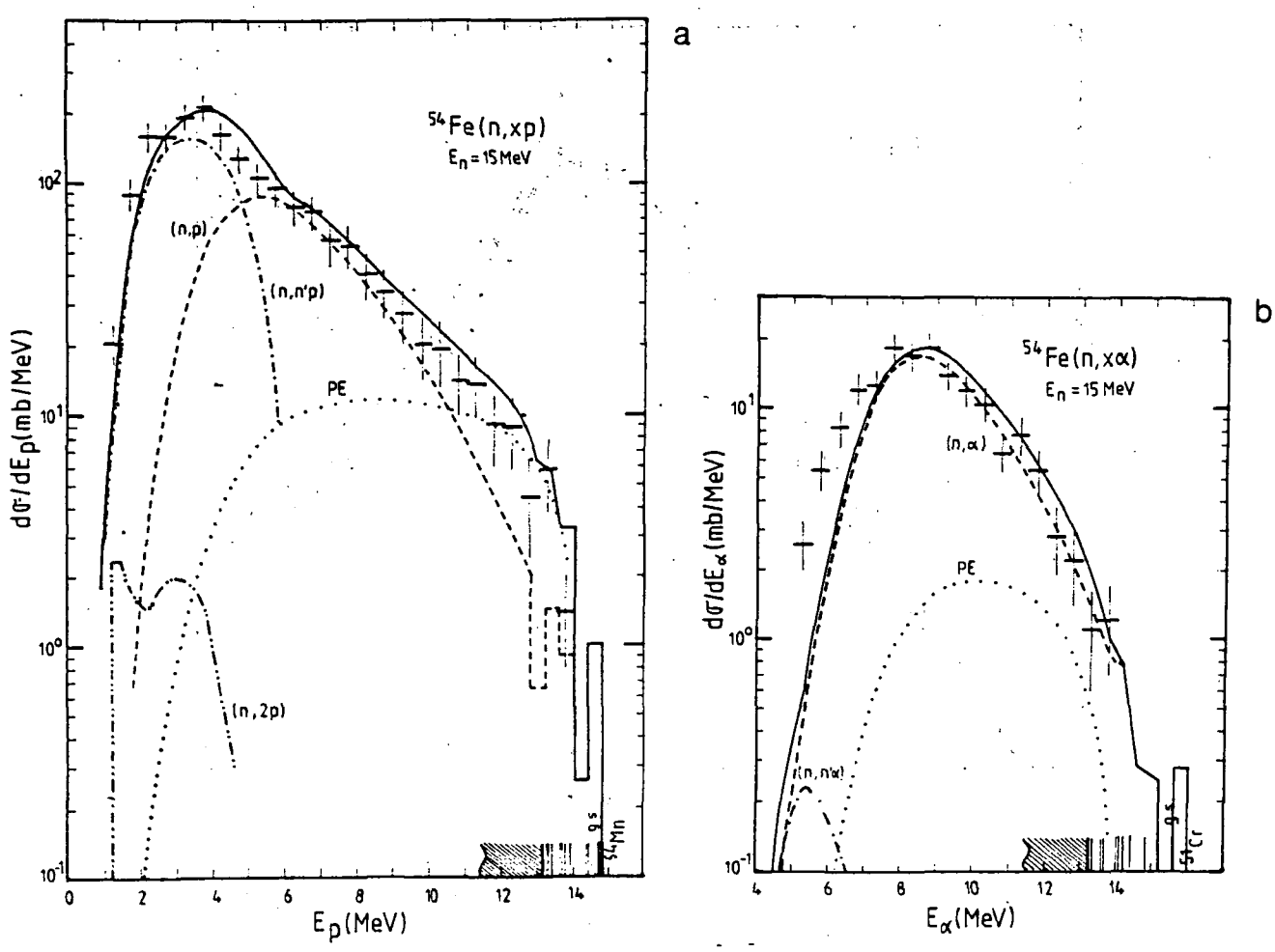

Fig. 4. Comparison of experimental [29] proton (a) and alpha-particle (b) emission spectra from 14.8 MeV neutron induced reactions on ^{54}Fe with calculated values by means of the pre-equilibrium emission generalized GDH model, including angular momentum and parity conservation, and Hauser-Feshbach statistical model (——). The various contributions shown are from: GDH (protons) or exciton (alphas) emission (....), first particle equilibrium emission (---), second particle emission (-.-). The anomalous low energy end of the (n, 2p) spectrum follows the separation energy difference $S_p - S_n \approx 1.4$ MeV in the compound nucleus ^{54}Mn. Between the calculated and experimental alpha particle spectra there is a shift because the calculations are in the center-of-mass system while the data are in the laboratory system (see also [50]).

the compound nucleus formation cross section. At the same time, following the GDH and Hauser-Feshbach calculation, the statistical (n,α) reaction cross section has been increased by σ^{α}_{PE}. The assumption of the whole alpha-particle pre-equilibrium emission contribution to the (n, α) channel has been based on the associated high E_α energies observed experimentally (around 12 MeV

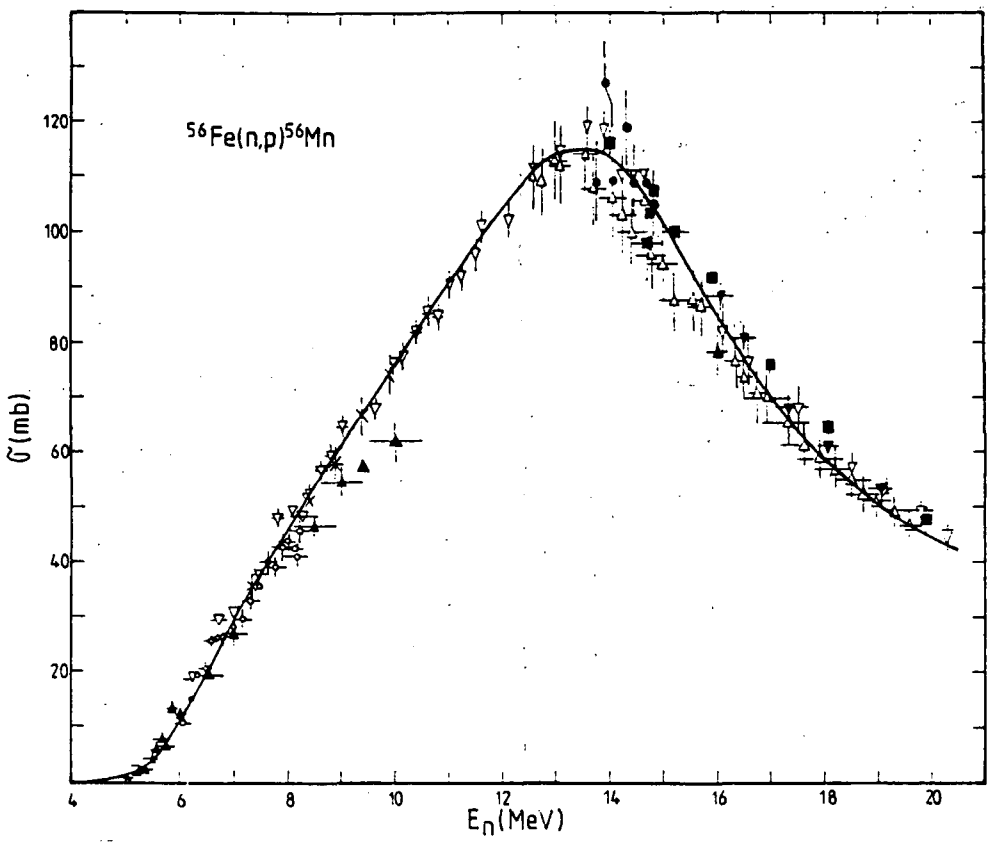

Fig. 5. Same as Fig. 1, for the reaction $^{56}Fe(n, p)^{56}Mn$. Experimental data: ▽ [51], △ [52], o [53], ▲ [35], ✱ [31], ▼ [48], ✖ [38], • [41], ■ [54].

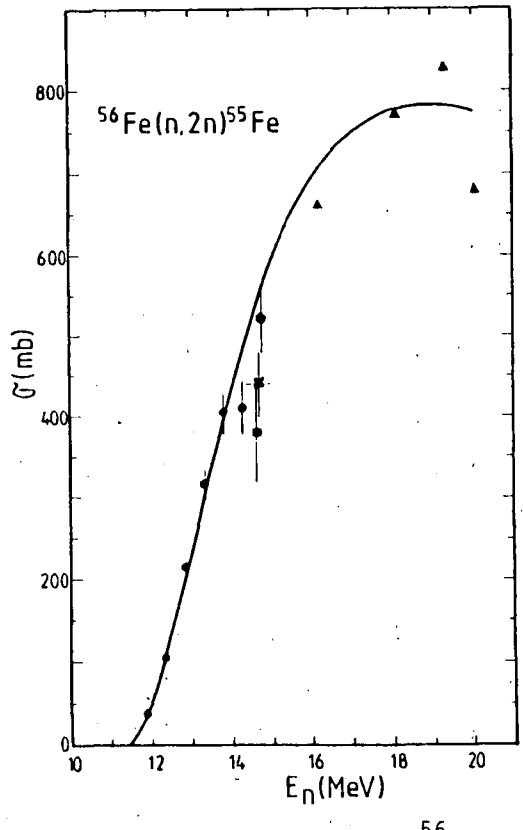

Fig. 6. Same as Fig. 1, for the reaction $^{56}Fe(n, 2n)^{55}Fe$. Experimental data: • [55], ✱ [56], ■ [57], ▲ [58].

[19]). Irrespective of this contribution, the statistical emission is well describing the experimental data up to $E_n \approx 10$ MeV (Fig. 2a). An important factor in achieving this was the use of the McFadden and Satchler OMP [22], increasing the (n, α) reaction cross sections by ≈30% with reference to other parameter set [18].The agreement between calculations and experiment at higher energies is also shown by the analysis of the alpha particle emission spectra (Figs. 4b, 7c),from which the probability value $\varphi = 0.3$ has been derived in the generalized GDH model.However, the decreasing validity of the above method using the fraction f^{α}_{PE} with the incident energy increasing is proved by the results of the generalized GDH model (Fig. 2b).

The study of the *neutron* and *proton emission spectra* (Figs. 4, 7) thus follows the validation of the nuclear level densities and the particle and γ - ray transmission coefficients. Consequently, the spectra resulting from the convolution of contributions from more channels may help in substantiated the pre-equilibrium emission model too. While the low energy end of these spectra is pointing out the correct accounting of the second particle emission, the middle part mainly corresponds to the first particle statistical emission and the higher energy part is related to the pre-equilibrium emission (separate contributions are depicted in Figs. 4,7). It is worthy of note that even the low energy or middle parts may be affected by the pre-equilibrium process, through the alteration of the high excitation first residual nucleus population (in the other channel) or of the first compound nucleus initial population (statistically de-excitating in the same channel). Therefore, the rather good agreement of the calculated spectra with the experimental data not only in the secondary high energy range, where the pre-equilibrium emission is the dominant process, but at all energies is validating the GDH model used.

Inclusion of the angular momentum and parity conservation in the GDH model allows for the proper comparison of the pre-equilibrium and statistical processes. The study of the *emission cross-section distribution* along the *composite system angular momentum* (e.g. Fig. 8) shows the pre-equilibrium component more or less localized at the high J-values end. As the ground state spin for the both $^{54,56}Fe$ target nuclei is zero, results that the pre-equilibrium emission originates from high ℓ_{inc}-value induced processes. Involving of the higher angular momenta is strengthening

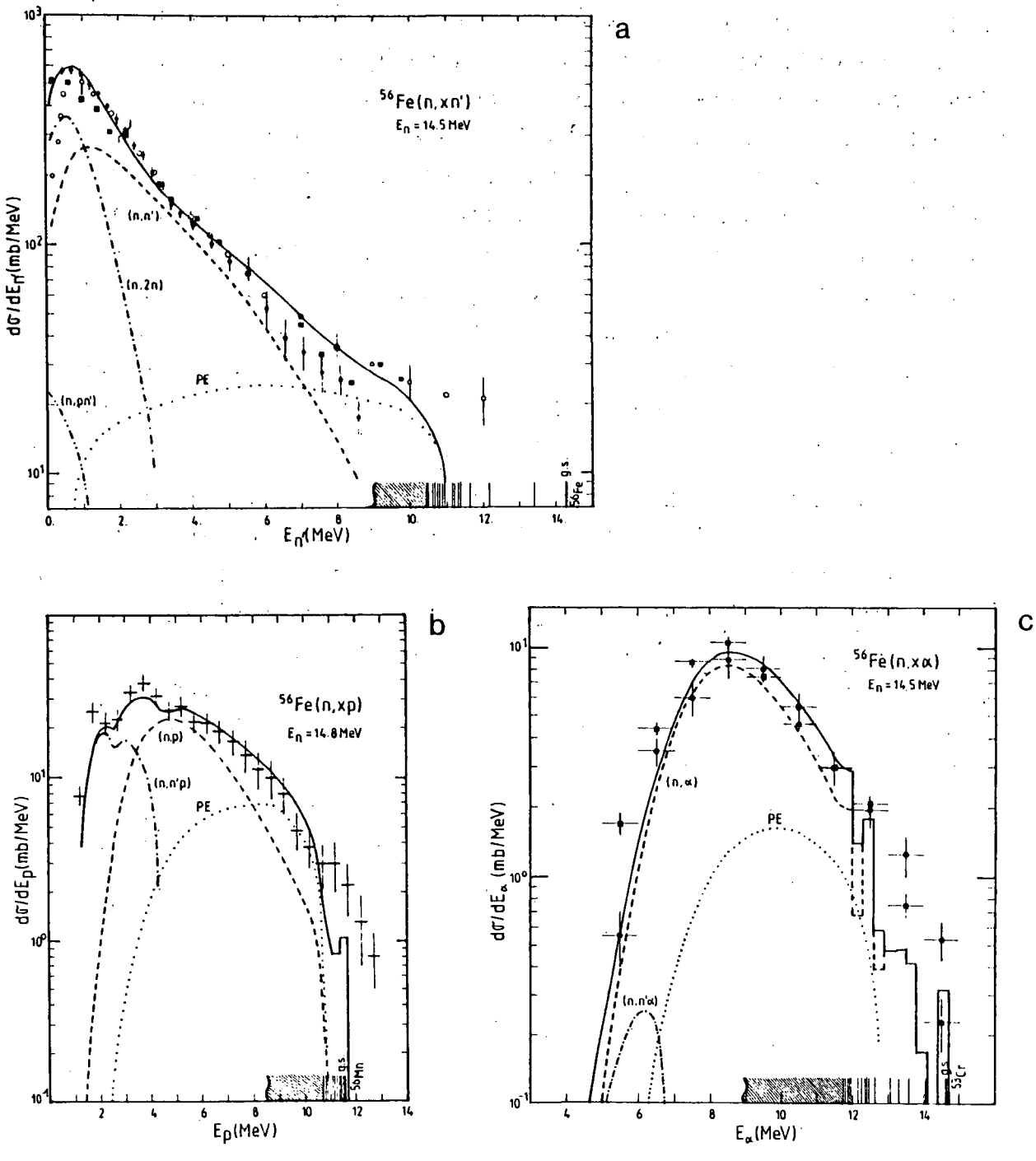

Fig. 7. Same as Fig. 4, for the neutron (a), proton (b) and alpha particle (c) emission spectra from the target nucleus ^{56}Fe. Experimental data: (a): • [59], o - averaged values [60], ■ [60]; (b): ⊸ [29]; (c): • [29] - transformed in the center-of-mass system [50], ■ [50]. The picture of the discrete levels taken into account in the calculations (the vertical lines above abscisa) evidences the necessity to include in such analyses also contributions from direct-reaction neutron inelastic scattering.

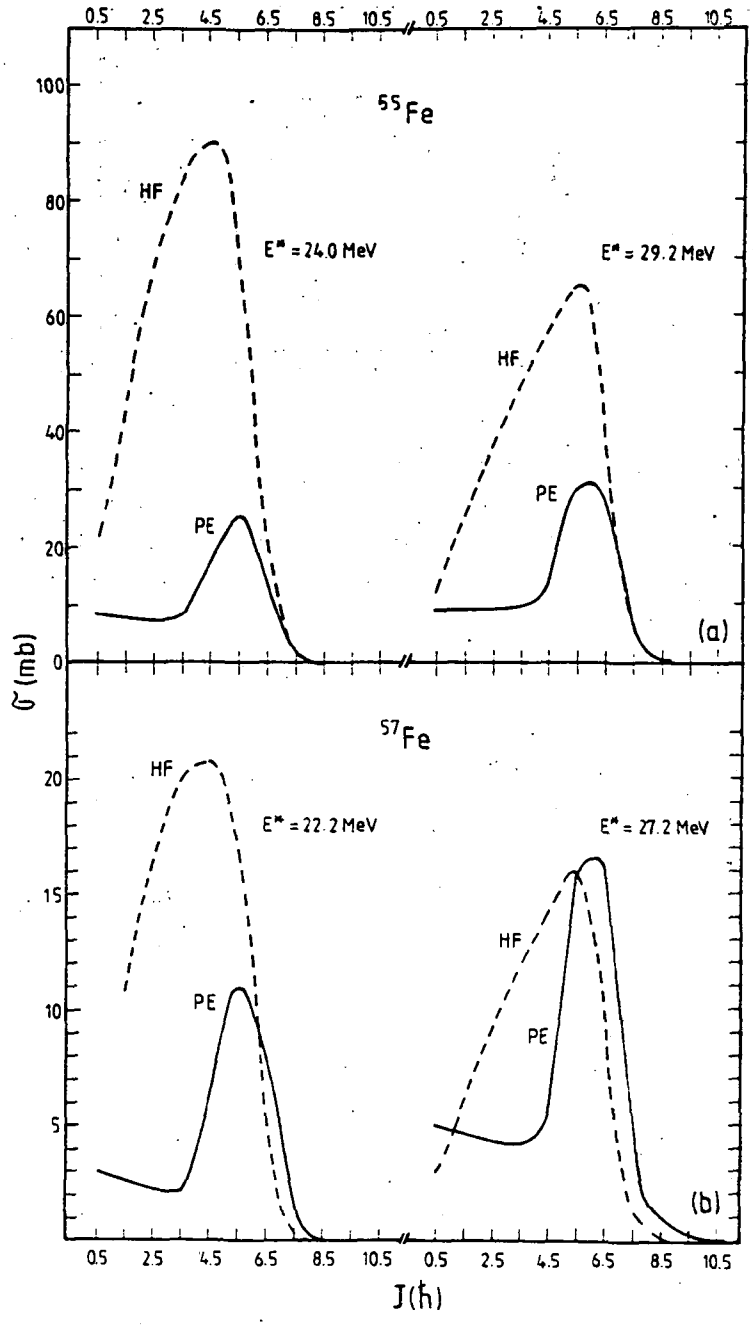

Fig. 8. The distributions of the pre-equilibrium (PE) and statistical Hauser-Feshbach (HF) proton emission cross sections along the composite system angular momentum J, for the systems ^{55}Fe(a) and ^{57}Fe (b) at different excitation energies E^* resulting from neutron induced reactions at E_n = 14.8 and 20 MeV.

the representation of the pre-equilibrium stage through predominant surface reactions, as suggested Shi Xiangjun et al. [30]. The more pronounced result for the proton emission from ^{57}Fe compound nucleus (Fig. 8b) arise due to the increase of the pre-equilibrium contribution to the (n, p) reaction cross section with the increasing of the asymmetry parameter (N-Z)/A. This aspect, largerly discussed elsewhere [9], is exemplified whithin the present calculations

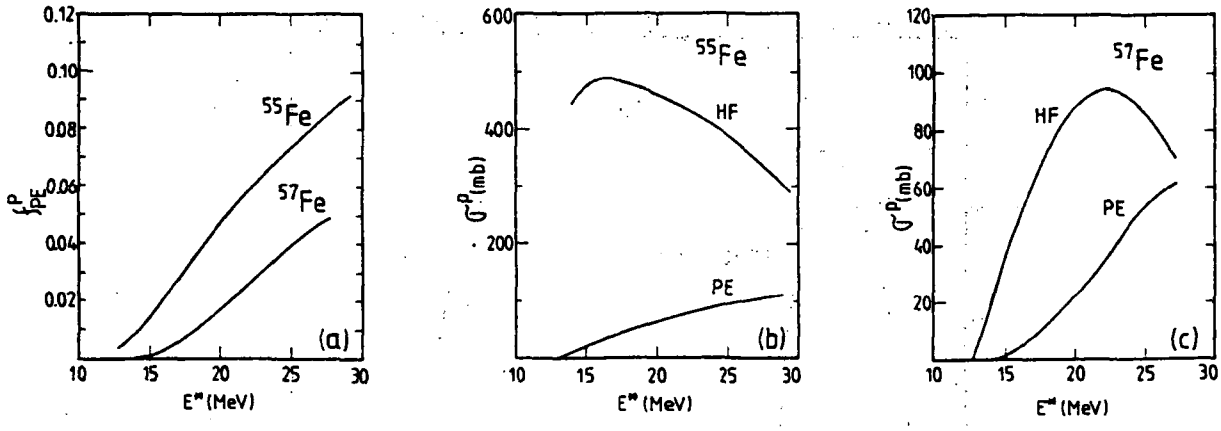

Fig. 9. The proton pre-equilibrium emission fractions (a) and the pre-equilibrium (PE) and statistical Hauser-Feshbach (HF) proton emission cross sections (b-c), versus the composite system excitation energy, for the systems $^{55,57}Fe$.

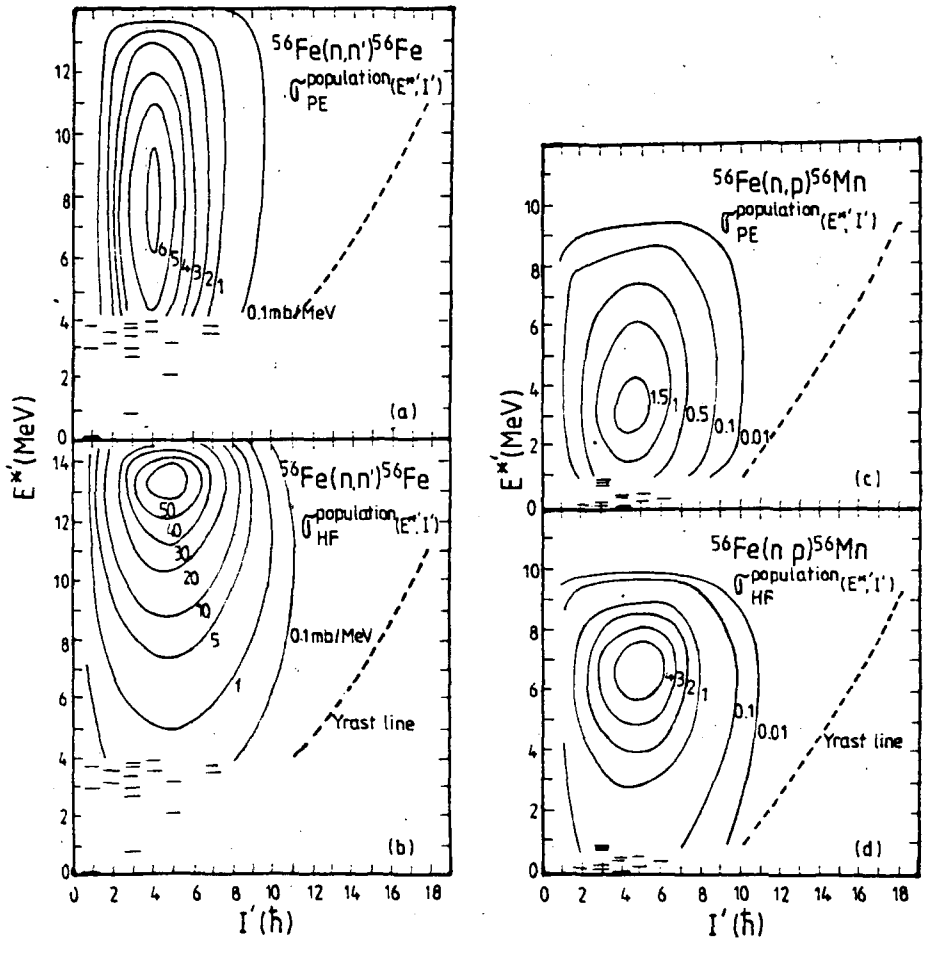

Fig.10. Nuclear level population cross sections (E^{*}', I') at excitation energies E^{*}' and level spins I', through pre-equilibrium (PE) and statistical Hauser-Feshbach (HF) emissions, for the residual nuclei ^{56}Fe (a-b) and ^{56}Mn (c-d) in the 14.8 MeV neutron induced reactions on ^{56}Fe.

in Fig. 9: the decreasing of the proton pre-equilibrium fraction $f^p_{PE} = \sigma^p_{PE}/\sigma_R$ with the asymmetry increasing (Fig. 9a) is exceeded by the statistical emission decreasing (Fig. 9 b-c) (the latter trend being mainly establishing the known "isotope effect" [31]). From both Figures 8 and 9 comes out that the enhanced pre-equilibrium emission from higher spin composite system states is also more pronounced with excitation energy increasing.

The calculation of the *residual nuclei level populations* through the two different mechanisms completes the present analysis. The yrast diagrams of these populations (Fig. 10) evidence maxima of the population cross sections following the pre-equilibrium emission appearing at smaller residual level spin values, relative to the similar maxima for the statistical process. Therefore, the pre-equilibrium emission is characterized by higher orbital momenta in the emergent channels, too. This aspect can be related to the experimentally observed hard particle emission spectra.

4. Cr ISOTOPES

4.1. NUCLEAR MODEL PARAMETERS

The consistent set of statistical model input parameters used in the cross section calculations for Cr isotopes has been established similarly to that employed for Fe isotopes. A special comment requires the OMP parameters used for calculation of the neutron and proton transmission coefficients.

Recent studies of fast neutron scattering on Cr are those of Guenther et al. [61] and Korzh et al. [62]. In the former an OMP has been derived based on total and elastic and inelastic scattering data in the neutron energy range from 1. to 4.5 MeV. In the latter the global OMP parameter set of Pasechnik et al. [63] has been used for neutron energies up to 9 MeV. However, both OMPs are predicting total cross sections higher than the experimental data for $E_n \lesssim 1.5$ MeV. An alternative OMP has appeared to be that of Engelbrecht and Fiedeldey [64] which is an extension of parameter set obtained by Moldauer [65] in an extensive analysis of s-wave strength functions, total cross sections for energies $E_n \lesssim 1$ MeV and scattering data, in the $A \simeq 40 - 150$ mass region. Nevertheless also these OMP predictions are overestimating the total cross sections on Cr below $E_n \simeq 1.5$ MeV. Finally,these data have been rathter well reproduced taking the constant real and imaginary depths of the Engelbrecht-Fiedeldey OMP $V_0 = 44$ and $W_0 = 10$ MeV as well as the real depth

radius $R_0 = (1.16\ A^{1/3} + 0.45)$ fm. The modified potential depths have approached the "asymptotic" values ($V_0 = 43$, $W_0 = 8$) obtained for the same OMP by Smith et al. [66] through the fit of elastic scattering data around $E_n = 1$ MeV on Vanadium.

Conclusively, the neutron transmission coefficients were calculated using the modified Engelbrecht-Fiedeldey OMP for $E_n \leq 1.0$ MeV and the OMP of Guenther et al. [61] at the higher energies. In doing so has been used the observation of a close relation between the compound nucleus cross sections given by [61] and the well known Studsvik global OMP [67] up to around 14 MeV.

The proton transmission coefficients were calculated using the BARC [20] global OMP above ≈4 - 5 MeV and the BARC [20] OMP with a variable imaginary depth W_D at lower energies. The W_D value has been chosen to allow the agreement between calculations and the experimental data for the low energy end of the (n, p) reaction excitation functions and sometimes also for the (n, n'p) peak of the proton spectra. Under such circumstances quite large W_0 value of 6 Me V has resulted.

Concerning the pre-equilibrium emission of the alpha-particles, it has been described only by means of the generalized GDH model.

4.2. RESULTS AND DISCUSSIONS

The large data base existing also for Cr isotopes has been analysed with view to the goals mentioned. The proton and alpha-particle emission spectra (Figs. 11, 12) have proved the accuracy of the generalized GDH model, as well as the correctness of the charged-particle transmission coefficients and the level densities at the medium excitation energy. On the other hand, the systematically underestimated high-energy end of the spectra emphasized the need to take into account the transfer direct interactions for a complete understanding of the fast neutron reaction mechanisms.

The analysis of the high energy part of the available (n,p) and (n, 2n) reaction excitation functions (Figs. 13-15) has contributed, together with the previously Fe data discussed and the Ni isotope investigation [28], to the establishing of the transition energy range limits for the mixed level density models employed. However, in the case of the Cr isotopes the (n, 2n) reaction excitation functions, most useful for this analysis, are less enlightening. The calculated $^{50}Cr\ (n,2n)^{49}Cr$ reaction excitation function shows a change of its slope due to the gaps in the low-level structure of

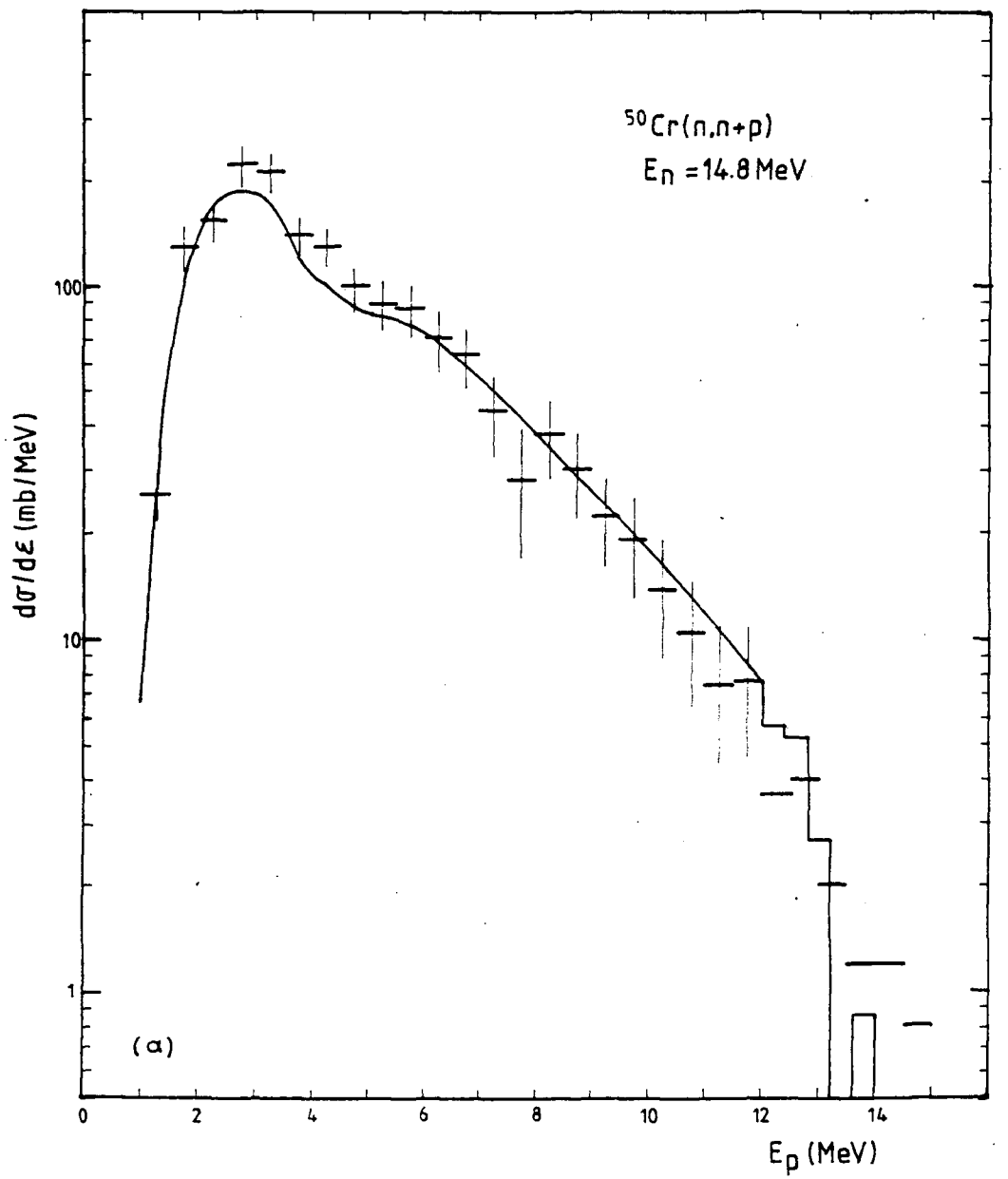

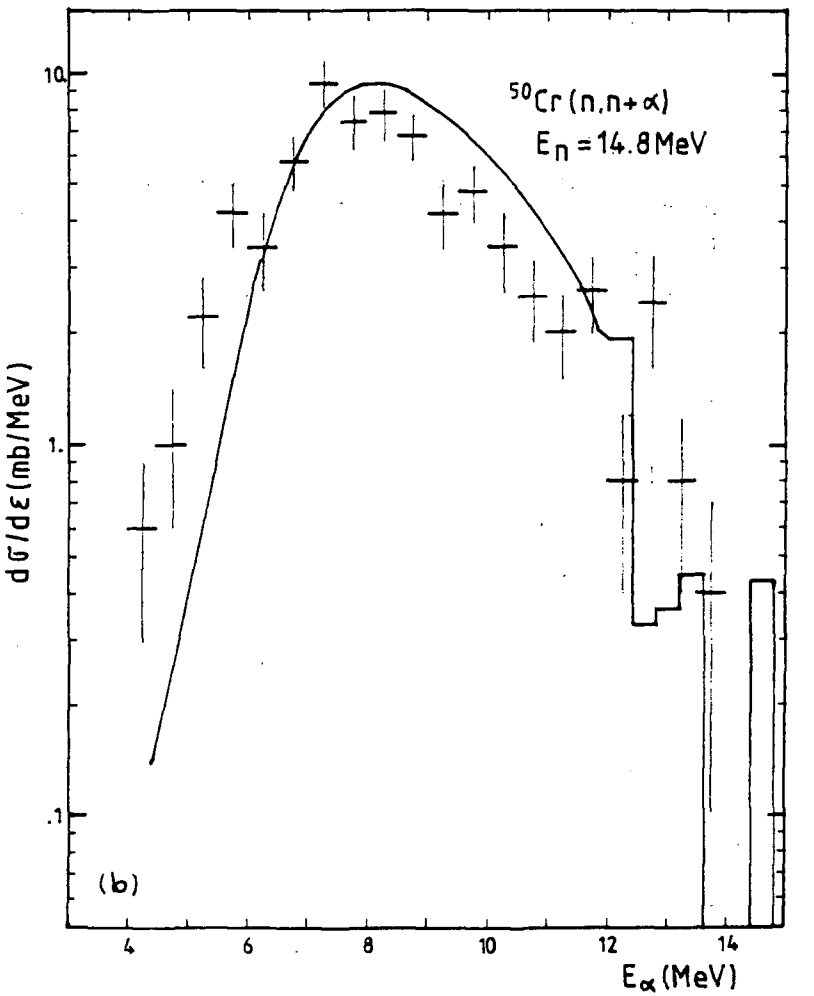

Fig. 11.
Same as Fig. 4, for the neutron (a) and proton (b) emission spectra from the target nucleus ^{50}Cr.

Fig. 12. Same as Fig. 4, for the neutron (a) and proton (b) emission spectra from the target nucleus ^{52}Cr.

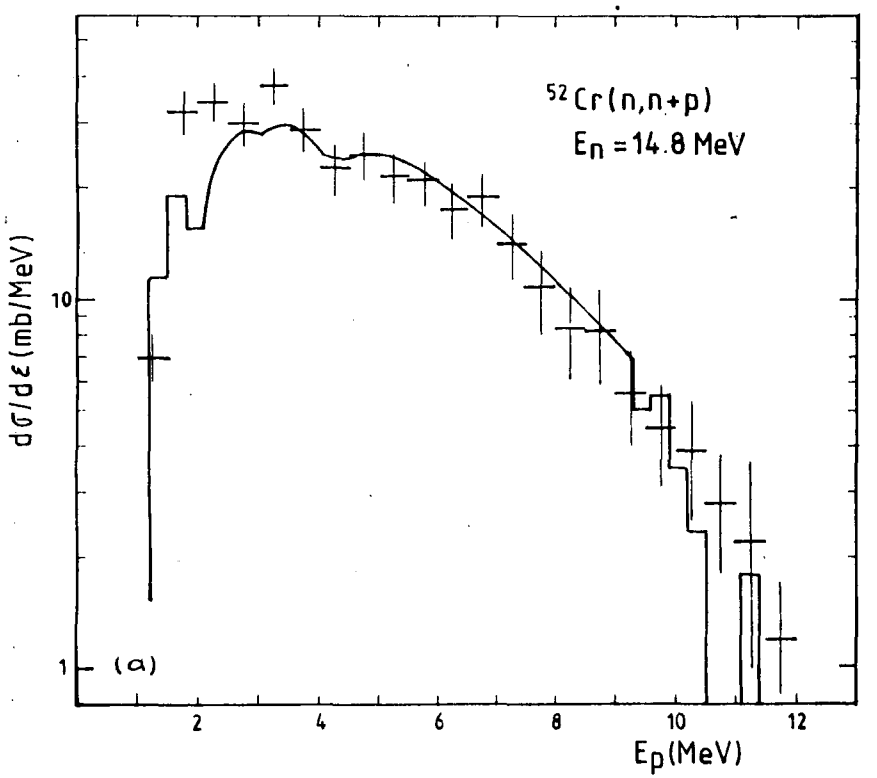

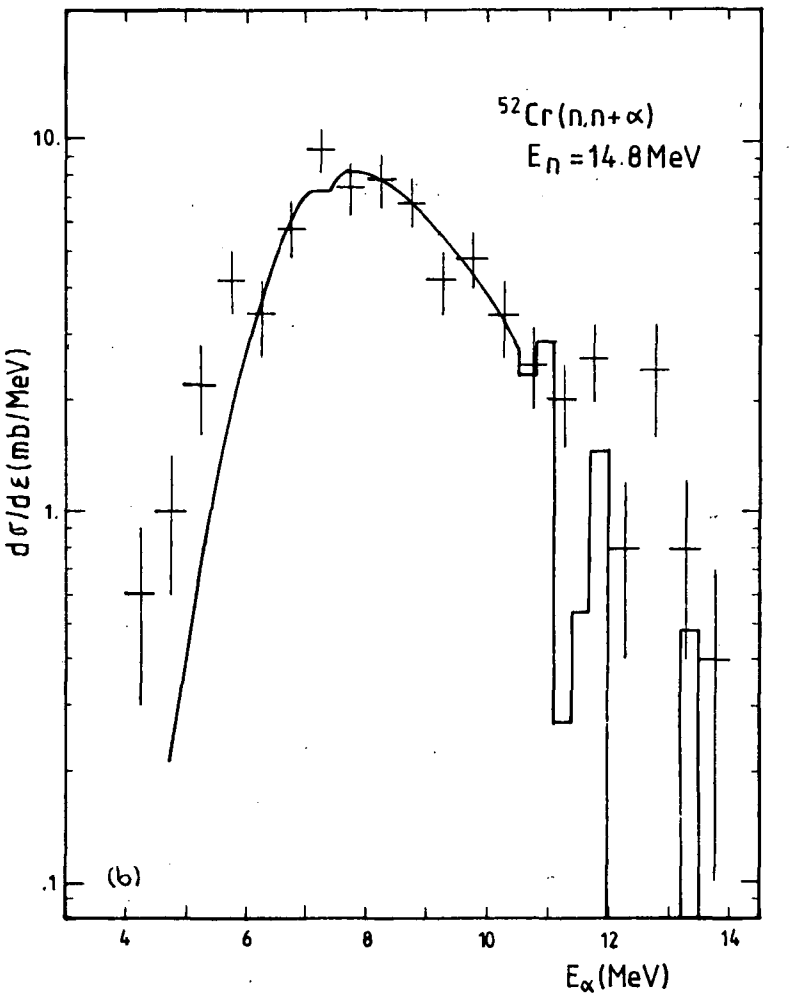

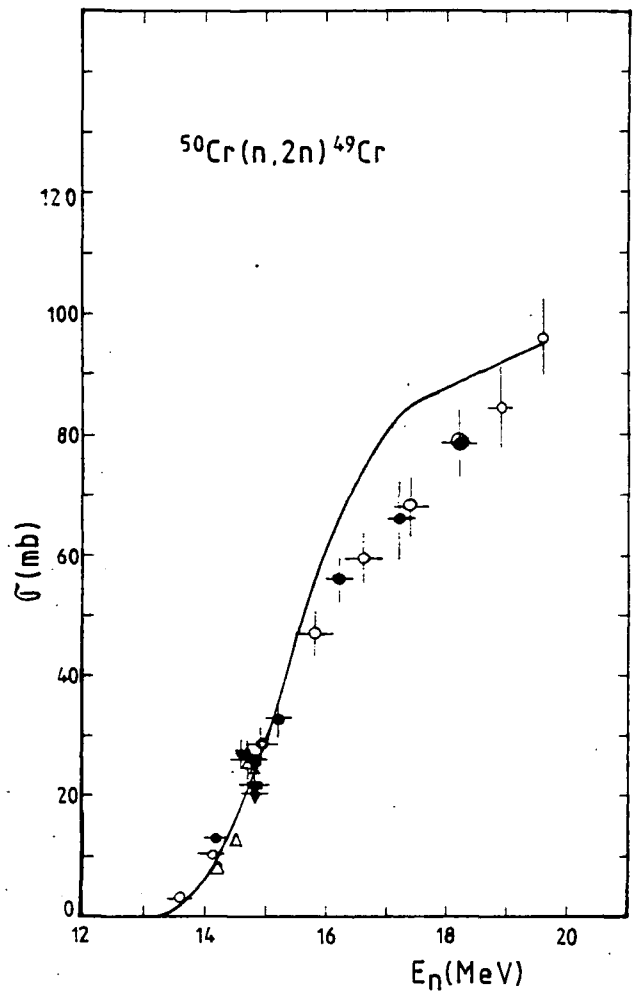

Fig. 13.
Same as Fig. 1, for the reaction $^{50}Cr(n, 2n)^{49}Cr$.
Experimental data: o [68], △ [69], ⊠ [33], ✱ [70], ■ [71], ▬ [72], ▼ [73], ▲ [44], ● [74], ♦ [75].

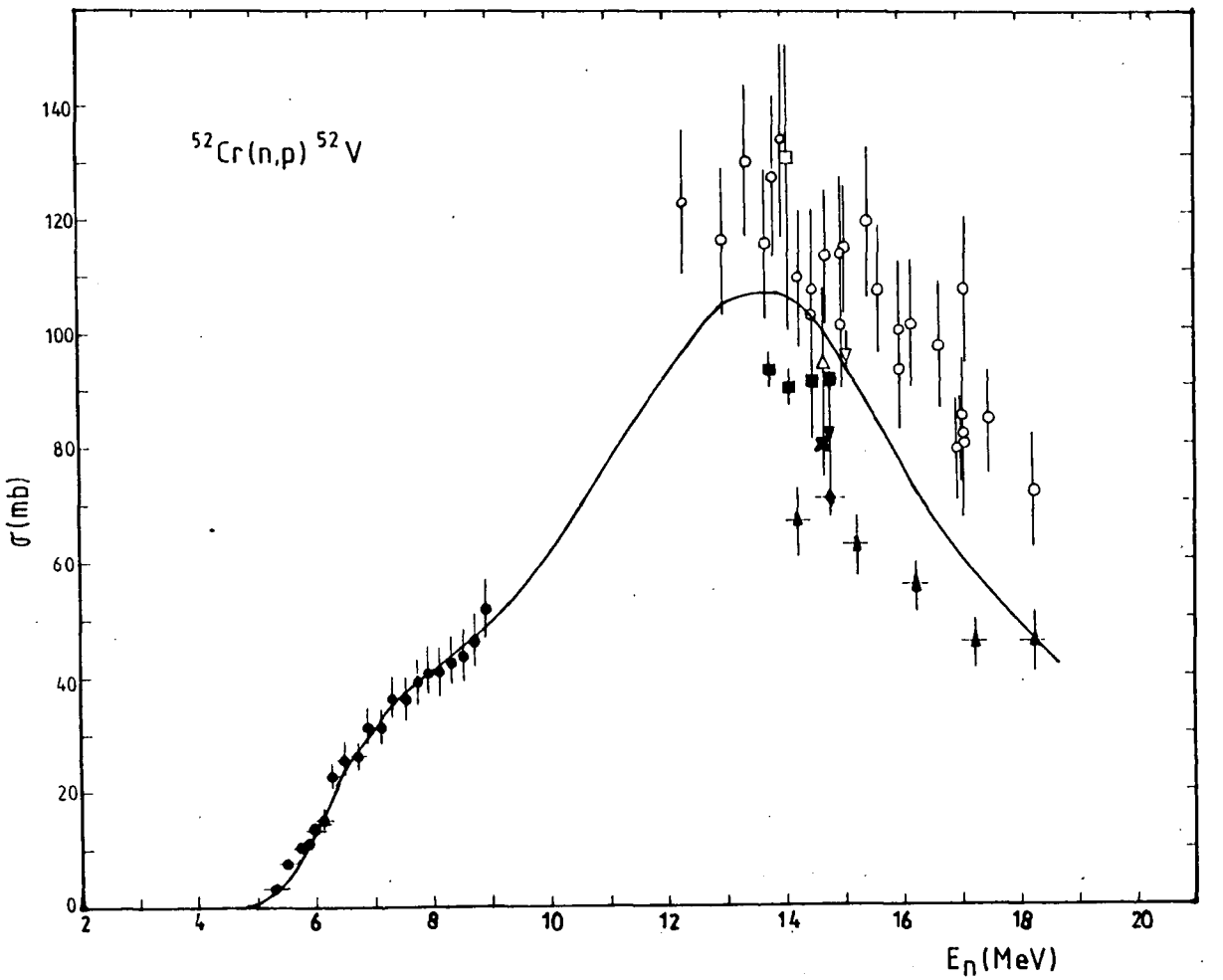

Fig. 14. Same as Fig. 1, for the reaction $^{52}Cr(n, p)^{52}V$.
Experimental data: o[76], ▽ [77], □ [78], ✱ [56], ● [79], ■ [41], ▼ [80], ♦ [75], ▲ [74].

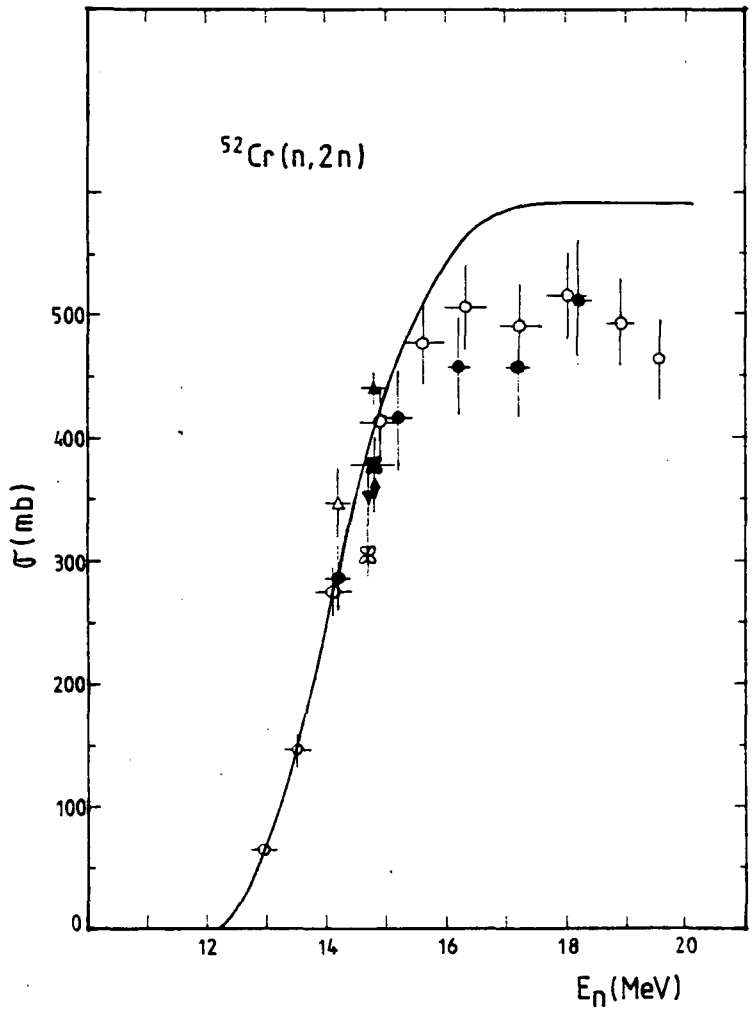

Fig. 15. Same as Fig. 1, for the reaction ^{52}Cr(n, 2n)^{51}Cr. Experimental data: o [81], ⊠ [45], △ [82], ▲ [72], ▼ [71], ✱ [83], ♦ [75], • [74].

the ^{49}V nucleus and is not too much affected by the variations of the transition limits. On the other hand, the calculated ^{52}Cr(n, 2n)^{51}Cr reaction excitation function is overestimating the higher energy data. Possible reasons might be an improper known compound nucleus cross section or the effect of direct interactions not taken into account. Nevertheless, also these data seem to support the transition range ≈10 - ≈35 MeV given by the Fe and Ni data analyses.

C O N C L U S I O N S

The generalized GDH pre-equilibrium emission model, along with the Hauser-Feshbach statistical model, is able to reliably account for a large body of related experimental data, without use of any free parameter. The significance of this aspect is

pointed out by the rather extended range of the values taken by the free parameter K of the exciton pre-equilibrium model in various studies [32].

The inclusion of the angular momentum and parity conservation in the GDH model has allowed the consistent connection of this model with the Hauser-Feshbach statistical model. Moreover, it allows the study of the pre-equilibrium emission process with reference to the populated states. Thus, an enhanced pre-equilibrium emission from the higher spin composite system states has been evidenced. The effect is more pronounced for higher asymmetry parameter values and higher excitation energies. Conclusively, this emission is associated with the higher incoming orbital momenta and, therefore, with predominant surface reactions. From the calculation of the residual nuclei level populations results that higher orbital momenta are also involved in the emergent channels of this process. This remark is well correlated with the hard experimental pre-equilibrium emission spectra.

While the analysis of the charged-particle spectra have validated the generalized GDH model, comparisons of the experimental and calculated (n, p) and (n, 2n) reaction excitation functions allow the establishment of the transition energy range limits characterizing the use of a semi-empirical level density model at medium excitation energies and of a realistic one at higher excitations. Following analyses of Fe, Cr and Ni data the transition range ≈10 - ≈35 MeV is obtained.

Achnowledgements are made to Dr. G.Semenescu for stimulating discussions on non-equilibrium processes. This work has been carried out under the contract 63-84-34 with the State Committee for Nuclear Energy, Bucharest, and under the research contract 3802/R2/RB between IPNE and International Atomic Energy Agency, Vienna.

R E F E R E N C E S

[1] Blann, M., Vonach, H.K.: Phys.Rev. C28, 1475 (1983)
[2] Hauser, W., Feshbach, H.: Phys.Rev. 87, 366 (1952)
[3] Moldauer, P.A.: Phys.Rev. 135, B642 (1964)
[4] Ivaşcu, M., Avrigeanu, M., Avrigeanu, V.: Rev.Roum.Phys. 32 713 (1987)
[5] Ivaşcu, M., Avrigeanu, V., Avrigeanu, M.: Rev.Roum.Phys. 32, 697 (1987)
[6] Avrigeanu, M., Avrigeanu, V., Căta, G., Ivaşcu, M.: Rev. Roum.Phys. 32, 837 (1987)

[7] Avrigeanu, M., Ivaşcu, M., Avrigeanu, V.: Report NP-63-1987, IPNE Bucharest, 1987, and Refs. therein.
[8] Milazzo-Colli, L., Braga-Marcazzan, G.M.: Nucl.Phys. A210, 297 (1973)
[9] Gadioli, E., Gadioli Erba, E., Hogan, J.J.: Phys.Rev. C16, 1404 (1977)
[10] Ferrero, A., Gadioli, E., Gadioli Erba, E., Iori, I., Molho, I., Zetta, L.: Z.Phys. A293, 123 (1979)
[11] Fu, C.Y.: Nucl.Sci.Eng. 92, 440 (1986)
[12] Akkermans, J.M., Gruppelaar, H.: Z.Phys. A321, 605 (1985)
[13] Chevarier, A., Chevarier, N., Demeyer, A., Alevra, A., Dumitrescu, R., Lukas, I.R., Magda, M.T., Nistor, M.E.: Nucl.Phys. A231, 64 (1974)
[14] Dilg, W., Schantl, W., Vonach, H., Uhl, M.: Nucl.Phys. A217, 269 (1973)
[15] Schmidt, K.-H, Delagrange, H., Dufour, J.P., Cârjan, N., Fleury, A.: Z.Phys.A - Atoms and Nuclei 308, 215 (1982)
[16] Ignatyuk, A.V., Smirenkin, G.N., Tishin, A.S.: Yad.Fiz. 21, 485 (1975)
[17] Delagrange, H., Benachou, A., Hubert, F., Llabador, Y., Heusch, B., Coffin, J.P., Engelstein, P., Fintz, P., Guillaume, G.: Nucl.Phys. A429, 173 (1984)
[18] Arthur, E.D., Young, P.G.: Report LA-8626-MS (ENDF-304) (1980)
[19] El-Kadi, S.M., Nelson, C.E., Purser, F.O., Walter, R.L., Beyerle, A., Gould, C.R., Seagondollar, L.W.: Nucl.Phys. A390, 509 (1982)
[20] Kailas, S, Mehta, M.K., Gupta, S.K., Viyogi, Y.P., Ganguli, N.K.: Phys.Rev. C20, 1272 (1978)
[21] Perey, F.G.: Phys.Rev. 131, 745 (1963)
[22] McFadden, L., Satchler, G.R.: Nucl.Phys. 84, 177 (1966)
[23] Vonach, H., Haight, R.C., Winkler, G.: Phys.Rev. C28, 2278 (1983)
[24] Huizenga, J.R., Igo, G.R.: Nucl.Phys. 29, 462 (1962)
[25] Avrigeanu, M., Avrigeanu, V., Cătă, G., Ivaşcu, M.: Rev.Roum.Phys. (in press)
[26] Gardner, D.G.: Report UCRL - 87438 (1982)
[27] Wapstra, A.H., Bos, K.: Atomic Data and Nuclear Data Tables 19, 177 (1977)
[28] Ivaşcu, M., Avrigeanu, M., Avrigeanu, V.: (to be published)
[29] Grimes, S.M., Haight, R.C., Alvar, K.R., Barschall, H.H., Borchers, R.R.: Phys.Rev. C19, 2127 (1979)
[30] Xiangyun, Shi, Gruppelaar, H., Akkermans, J.M.: Report ECN-85-133 (1986)
[31] Molla, N.I., Qaim, S.M.: Nucl.Phys. A283, 269 (1977)
[32] Jahn, H.: Report KfK - 3646 (1984)
[33] Qaim, S.M., Wölfle, R., Stöcklin, G.: Proc.Int.Conf. Chemical Nuclear Data, Caterbury, 1971, pp. 121
[34] Paulsen, A.A., Widera, R.: Proc.Int.Conf.Chemical Nucl.Data, Caterbury, 1971, pp. 129

[35] Smith, D.L., Meadows, J.W.: Nucl.Sci.Eng. 58, 314 (1975)
[36] Ai, O.E., Wu, M.W., Chou, J.C.: Nucl.Sci.J. 14, 1 (1977)
[37] Fukuda, K., Matsuo, K., Shirahama, S., Kumabe, I.: Report NEANDC (J)-56/U (1978), pp. 44
[38] Paulsen, A.A., Widera, R., Arnotte, F., Liskien, H.: Nucl.Sci.Eng. 72, 113 (1979)
[39] Klochkova, L.I., Kovrigin, B.S., Kuricyn, V.N., Lavrova, N.S., Cherepanov, E.V., Shibajev, V.A.: Proc.5th All Union Conf. on Neutron Physics, Kiev, 1980, pp. 53
[40] Lu Han-Lin, Li Ji-Zhou, Fan Pei-Guo, Huang Jian-Zhou: Chinese J. of Nucl.Phys. 4, 272 (1982)
[41] Viennot, M., Haddou, A., Chiadli, A., Paic, G.: Proc.Int. Conf. on Nucl.Data for Science and Technology, Antwerp, 1982, pp. 406. Dordrecht: Reidel Publishing Comp., 1983
[42] Calamand, A., Lemmel, H.D.: Report IAEA-NDS-1, Rev.4 (1983), EXFOR data received from IAEA Nuclear Data Section, Vienna.
[43] Salisbury, S.R., Chalmers, R.A.: Phys.Rev. 140B, 305 (1965)
[44] Bahal, B.M., Pepelnik, R.: Report NEANDC(E)-252/U (1984), pp.5
[45] Qaim, S.M.: Nucl.Phys. A185, 614 (1972)
[46] Sigg, R.A., Kuroda, P.K.: J.Inorg.Nucl.Chem. 37, 631 (1975)
[47] Bormann, M., Fedderson, H.K., Holscher, H.H., Scobel, W., Wagner, H.: Z.Phys.A - Atoms and Nuclei 277, 203 (1976)
[48] Ryves, T.B., Kolkowski, P., Zieba, K.J.: J.Phys.G: Nucl. Phys. 4, 1783 (1978)
[49] Ryves, W.: Data File EXFOR-20772.002 dated 1978-11-02. EXFOR data received from IAEA Nuclear Data Section, Vienna.
[50] Fischer, R., Traxler, G., Uhl, M., Vonach, H.: Phys.Rev. C30, 72 (1984)
[51] Santry, D.C., Butler, J.P.: Can.J.Phys. 42, 1030 (1964)
[52] Liskien, H., Paulsen, A.: J.Nucl.En. 19, 73 (1965)
[53] Liskien, H., Paulsen, A.: Nukleonika 8, 315 (1966)
[54] Kudo, K.: Data file EXFOR-21923.003 dated 1985-01-29
[55] Frehaut, W., Bertin, A., Bois, R., Jary, J.: Data file EXFOR-20416.003 dated 1975-07-28
[56] Qaim, S.M., Molla, N.I.: Proc.9th Symp. on Fusion Technology, Garmisch-Partenkirchen, 1976, pp.589. Oxford: Pergamon Press 1976
[57] Kozyr, I.E., Pljujko, V.A., Prokopets, G.A.: Proc.4th All Union Conf.on Neutron Physics, Kiev, 1977, pp. 256
[58] Corcalciuc, V., Holmqvist, B., Marcinkowski, A., Prokopets, G.A.: Nucl.Phys. A307, 445 (1978)
[59] Stengl, G., Uhl, M., Vonach, H.: Nucl.Phys. A290, 109 (1977)
[60] Lychagin, A.A., Simakov, S.P., Devkin, B.V., Salnikov, O.A., Androsenko, A.A., Androsenko, P.A., Paschchenko, A.B., Grudzevich, O.T., Peto, G., Starichkai, T., Vashvari, L.: Yad.Fiz. 45, 1226 (1987).

[61] Guenther, P.T., Smith, A.B., Whalen, J.F.: Nucl.Sci.Eng. 82, 408 (1982)
[62] Korzh, I.A., Mishchenko, V.A., Mozhzukhin, E.N., Pravdivyl: Yad.Fiz. 35, 1097 (1982)
[63] Pasechnik, M.V., Korzh, I.A., Kashuba, I.E.: in Neitronnaya Fizika, Kiev, Naukova dumka, 1972, part. 1, p. 253.
[64] Engelbrecht, C.A., Fiedeldey, H.: Ann.Phys. 42, 262 (1967).
[65] Moldauer, P.A.: Nucl.Phys. 47, 65 (1963)
[66] Smith, A.B., Whalen, J.F., Takeuchi, K.: Phys.Rev. C1, 581 (1970)
[67] Holmqvist, B., Wiedling, T.: J.Nucl.Energy 27, 543 (1973)
[68] Bormann, M.: Data File EXFOR - 21525-002 dated 1965-01
[69] Chatterjee, A., Nath, A., Ghose, A.M.: Report BARC-474, 50 (19 (1970)
[70] Araminowicz, J., Dresler, J.: Report INR-1464, 14 (1973)
[71] Daroczy, S., Nagy, S., Petö, G., Raics, P., Sailer, K.: Report INDC (SEC)-61, IAEA-Vienna, 1977
[72] Sailer, K., Daroczy, S.: Proc. 4th All Union Conf. on Neutron Physics, Kiev, 1977, pp. 246.
[73] Berrada, M.: Prog.Rep. IAEA Research Contract 3311/R1/RB, 1983-1984
[74] Ghorai, S.K., Williams, J.R., Alford, W.L.: J.Phys.G.: Nucl.Phys. 13, 405 (1987)
[75] Ribanski, I.: Data File EXFOR-30812-002 dated 1985-03-20.
[76] Kern, B.D., Thompson, W.E., Ferguson, J.M.: Nucl.Phys. 10, 226 (1959)
[77] Dresler, J., Araminowicz, J., Garuska, U.: Report INR-1464, 12 (1973)
[78] Aleksandrov, D.V., Klochkova, L., Kovrigin, B.S.: At.Energy 39, 137 (1975)
[79] Smith, D.L., Meadows, J.W.: Nucl.Sci.Eng. 76, 43 (1981)
[80] Hoang Dac Luc: Report INDC (VN)-003, IAEA Vienna, 1984
[81] Bormann, M., Behrend, A., Riehle, I., Vogel, O.: Nucl.Phys. A115, 309 (1968)
[82] Maslov, G.N., Nasyrov, F., Pushkin, F.: Report YK-9, 1972
[83] Molla, N.I., Mizanul Islam, M., Mizanur Rahman, M., Khatun, S.: Report INDC (BAN)-002, IAEA-Vienna, 1983.